Diode Laser Measurements of Temperature and H_2O for Monitoring Pulse Detonation Combustor Performance

Christopher S. Goldenstein, Ian. A Schultz, R. Mitchell Spearrin, Jay B. Jeffries, and Ronald K. Hanson
Stanford University
Stanford, CA, USA

1 Introduction

Tunable diode laser absorption spectroscopy (TDLAS) sensors are a useful tool for providing non-intrusive, *in situ* measurements of gas temperature, composition, and bulk velocity [1]. Although TDL sensors are most commonly used in low-pressure (< 2 atm) applications such as scramjets and low-pressure shock tubes [1,2], some work has been conducted in high-pressure environments (e.g. internal combustion engines, gas turbines, pulse detonation combustors, and coal gasifiers) [3]. The thermodynamic benefits of high-pressure and high-temperature combustion have led to the development of several novel, high-pressure combustion systems that require high-bandwidth TDLAS diagnostics capable of operating at gas pressures and temperatures greater than 10 atm and 2000 K, respectively. As a result, a new generation of sensors tailored to the operating conditions of such high-pressure systems is required.

Pulse detonation combustors and engines (PDC/E) present a particularly challenging environment for TDL diagnostics. Such systems feature strong, rapid transients and extreme gas conditions (T = 500-4000 K and P=1-100 atm). As a result, TDL sensors suitable for PDC/E deployment must be optically robust, possess high-bandwidth (at least 1 kHz), and operate over a broad range of temperature and pressure space.

Here we present the design and demonstration of a TDLAS sensor for measuring temperature and H_2O mole fraction in high-pressure (2-50 atm) and high-temperature (600-3500 K) combustion gases. The sensor used a normalized wavelength-modulation spectroscopy (WMS) scheme to become insensitive to non-absorbing optical transmission losses and emission. Two-color thermometry was performed with water vapor transitions located near 1.4 μm, and the measured temperature was used to calculate H_2O mole fraction at the independently measured gas pressure; simultaneous absorption measurements of CO and CO_2 were also performed [4]. These multi-species TDLAS measurements were conducted across two orthogonal lines-of-sight (LOS) in the throat of a converging-diverging nozzle located at the exit of a PDC located at the Naval Postgraduate School (NPS) in Monterey, CA. By assuming that the flow was choked at the TDLAS measurement location, it is possible to calculate the choked bulk flow speed (i.e. sound speed) using only the TDLAS measured temperature and composition. With the local pressure, temperature, composition, and bulk speed known, the time-varying mass flow rate and stagnation enthalpy were calculated to monitor thermodynamic power output.

Correspondence to: csgolden@stanford.edu

2 Experimental Setup

NPS Pulse Detonation Combustor

The NPS PDC consists of a 1.3 m long, 3" diameter combustion chamber and a converging-diverging nozzle located at the combustor exit. The nozzle throat is 1.4" in diameter and the nozzle area ratio is 1.1. Six detonation obstacles were located within the combustor to promote the formation of fully-developed detonations. During operation, compressed air at 560 K and 5.75 atm was continuously fed into the combustor and ethylene was intermittently injected into the intake manifold in near-stoichiometric proportions at the beginning of each cycle.

TDLAS Sensor Hardware

Figure 1 displays a schematic of the TDLAS experimental setup. For temperature and H_2O sensing, two telecom-grade diode lasers near 1392 and 1469 nm were combined onto a single polarization maintaining (PM) fiber to deliver laser light to the PDC nozzle. The light was collimated and pitched across the nozzle throat. A 12 mm diameter focusing optic was used to collect and focus the transmitted light into a 450 µm multi-mode fiber (MMF). The MMF delivered light to an InGaAs photo-detector with a 7 mm^2 active area. The NIR lasers were modulated at 160 and 200 kHz with a modulation depth of 0.35 and 0.25 cm^{-1}, respectively. The detector signal was collected at 5 MHz and WMS harmonics were extracted with 10 kHz low-pass Lanczos filters during post-processing. A similar setup was used for the mid-IR CO_2 (2.7 µm) and CO (4.8 µm) lasers using appropriate mid-IR fibers [4].

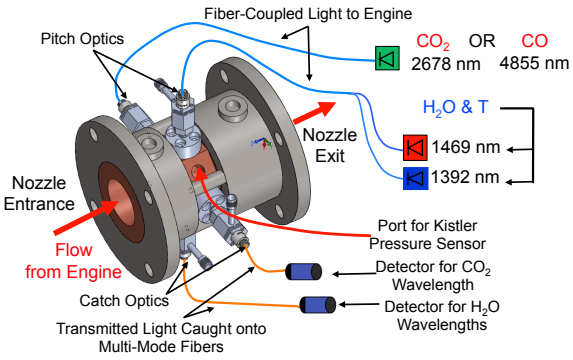

Figure 1. Experimental setup of TDL sensors mounted to NPS PDC nozzle throat.

3 Sensor Development

Diagnostic Strategy

In WMS, each wavelength-multiplexed laser is tuned in wavelength to a specific point on an absorption feature and sinusoidally modulated about that center wavelength at a given frequency, *f*. The interaction between the rapidly modulated laser wavelength and the absorption feature lineshape introduces frequency content in the transmitted laser light that is centered at the harmonics of the laser modulation frequency. These signals can be separated in frequency space via lock-in filters and compared with simulated signals to infer gas properties [5]. By employing 1*f*-normalization, the higher-harmonic signals (2*f*, 3*f*, 4*f*, *etc.*) become independent of the DC magnitude of the incident and collected light intensity. As a result, knowledge of the baseline laser intensity and non-absorbing optical losses are not required for quantitatively accurate WMS-2*f*/1*f* measurements. Furthermore, WMS-2*f*/1*f*

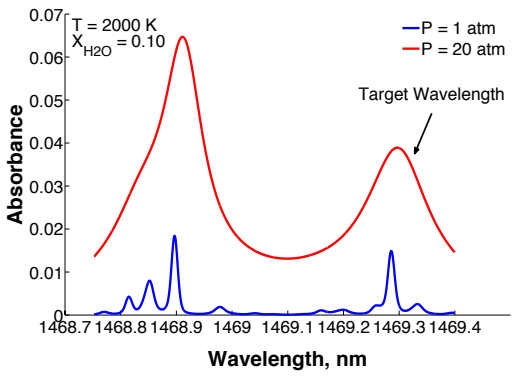

Figure 2. Simulated H_2O absorbance spectra near 1469 nm at 1 and 20 atm. High-pressure leads to broad and blended spectra.

suppresses interference from optical emission. More information regarding WMS can be found in the literature [6-7].

Here WMS-2*f*/1*f* was used for several reasons. 1) Recovery of baseline incident light intensity is problematic in harsh, high-pressure environments as a result of broad and blended absorption spectra and non-absorbing optical losses resulting from beam-steering, window fouling, and mechanical vibration. For traditional direct absorption measurements the laser is tuned to a non-resonant wavelength to determine a "non-absorbing baseline." While this can be done at low pressures, this strategy becomes problematic at high pressures due to collisional broadening. For example, Figure 2 shows that non-absorbing wavelengths exist near 1469 nm at 1 atm, but not at 20 atm. 2). In WMS-2*f*/1*f*, wavelength-multiplexed signals from multiple lasers are demultiplexed in frequency space. This technique enables the benefits of wavelength-multiplexed systems (e.g. simultaneous measurements along a single LOS with multiple wavelengths, common-mode noise rejection, and fewer optical components), without the complexity of wavelength demultiplexing or the loss of sensor bandwidth with time demultiplexing.

Wavelength Selection

Selecting appropriate wavelengths is critical to the success of all TDLAS sensors. In low-pressure gases, this processes largely consists of selecting well-isolated transitions with desirable strength and lower-state energy [8]. At high pressures, however, this strategy is complicated by collisional broadening which leads to broad and blended spectra. As a result, the absorbance and its temperature dependence at a given wavelength is dominated by the strength and broadening parameters of all nearby transitions.

For the work presented here, the laser wavelengths employed were those used previously in Goldenstein et al. [9], where wavelengths were selected based on the temperature-and pressure-dependent behavior of the complete pressure-broadened absorbance spectra, as opposed to only considering the behavior of individual transitions. The magnitude of absorbance, temperature sensitivity, and relative isolation from strong neighboring transitions of all potential wavelengths in the 1.4 μm absorption band were considered. These wavelengths and select spectroscopic properties of the dominant transitions were published previously [9].

Absorption Spectra Model Development

The ability to accurately model the absorbance spectra over the measurement domain is essential to the accuracy of all TDLAS sensors. This requires accurate spectroscopic parameters and lineshape models. As a result, a semi-empirical spectroscopic database was developed and validated in controlled experiments. Linestrengths, collisional-broadening parameters, pressure-shift coefficients, and their respective temperature exponents were measured in low-pressure, static-cell experiments from 600-1300 K and 0.1-1 atm. Scanned-wavelength direct absorption was used to measure transition linestrengths in neat H_2O mixtures, and collisional-broadening parameters were measured for H_2O, N_2, and CO_2 colliders. To refine the absorption spectra model developed via static-cell experiments, WMS-2*f*/1*f* measurements were conducted behind incident and reflected shock waves in H_2O-N_2 mixtures at high pressure (P = 2-25 atm) and high temperature (600-2300 K) in the Stanford High-Pressure Shock Tube (HPST) described in [10]. These high-pressure measurements were used for an improved determination of N_2-broadening coefficients and their respective temperature exponents for the two dominant transitions. This calibration step is necessary for two primary reasons. 1). The temperature exponent used to describe the power-law temperature dependence of collisional broadening coefficients is also slightly temperature dependent [11]. 2). In addition, collisional narrowing can introduce systematic errors in the collisional-broadening coefficients extracted from Voigt profile fits conducted in low-pressure experiments [12]. While alternative lineshape profiles (Galatry, Rautian, Soble'man etc.) can be fit to collisionally narrowed lineshapes to address this problem, the additional fitting parameters required by these lineshape functions can compromise the

accuracy of all lineshape parameters extracted from the data. This refinement of lineshape parameters in a controlled high-pressure and high-temperature environment enables high-fidelity, calibration-free measurements in uncontrolled field experiments.

Sensor Validation

Measurements were conducted at high pressure and high temperature in the Stanford HPST to validate the sensor's accuracy. During each test, measurements were acquired across two LOS located 2 cm and 95 cm from the shock tube endwall to interrogate the gas located behind the incident and reflected shock. Measurements at pressures below 8 atm were acquired behind the incident shock. The sensor's performance is summarized in Figure 3 where measured values are compared with known quantities. The known temperature was calculated using shock-jump relations [13] and measured shock speeds, and the known H_2O mole fraction was determined from scanned-wavelength direct-absorption experiments conducted in the test mixture prior to the arrival of the incident shock. The data in Figure 3 demonstrates that the sensor provides accurate thermometry and H_2O sensing at temperatures and pressures ranging from 600-2300 K and 2-25 atm. The quoted values represent mean values and error bars represent one standard deviation during the 0.5-2 ms steady-state test time.

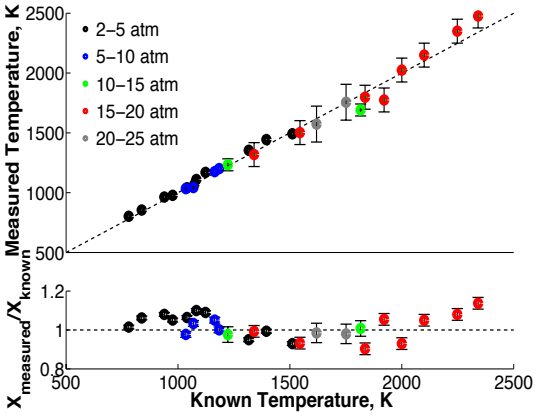

Figure 3. Performance summary of measured temperature (top) and H_2O mole fraction (bottom) as a function of known temperature at pressures ranging from 2-25 atm.

4 NPS PDC Results

Results

Pressure, temperature, and H_2O mole fraction results for data collected over an entire PDC cycle are presented in Figure 4. The measured peak temperature and pressure for this cycle was 3550 K and 48 atm, respectively. These extreme values and the presence of H_2O immediately behind the shock front in the throat suggests that a detonable mixture reached the PDC throat prior to the arrival of the shock front. As a result, the fuel injection timing was advanced to prevent this in future runs, since overfilling typically results in decreased fuel efficiency. Lastly, the H_2O time history illustrates several noteworthy trends. The H_2O mole fraction increased to near stoichiometric proportions (~13% by mole) between 0.5 and 2.5 ms before falling abruptly at the arrival of the compression fan. This rise and fall is a result of the time-varying equilibrium state of the gas and stratified fuel loading. The second, slight rise in H_2O mole fraction beginning near 3 ms resulted from the arrival of combustion products that continued to occupy the combustion chamber until the engine was completely purged 25 ms after ignition.

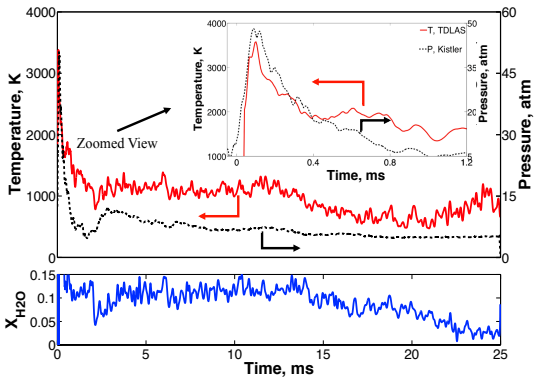

Figure 4. Measured pressure, temperature (top), and water mole-fraction (bottom) time histories for a PDC cycle.

Calculation of Engine Performance Metrics

The measurement of pressure, temperature, and composition in a choked throat enable the calculation of mass flow rate and stagnation enthalpy. Gas temperature and composition were calculated from WMS signals according to the methods outlined in Rieker et al. [5]. The mass flow rate and stagnation enthalpy were calculated as follows. A major products assumption was invoked with the following assumptions: all nitrogen existed in diatomic form, all oxygen existed in H_2O, CO, and CO_2, all hydrogen existed in H_2O, and all carbon existed in CO and CO_2. While minor species certainly existed, CFD simulations suggest that these four major species accounted for more than 97% of the gas composition by mole. The remaining 3% of the gas was treated as N_2. The ratio of specific heats was then calculated for all four dominant species at the measured temperature using the Burcat polynomials [15]. The sound speed of the flow was calculated using the measured temperature and ratio of specific heats of the mixture. The ideal gas law was used to calculate the local gas density at the measured temperature, pressure, and mixture gas constant. The mass-specific sensible enthalpy of the mixture was calculated relative to the reference temperature of 298 K using the Burcat polynomials. All mixture properties were calculated using conventional ideal-mixture relations. Lastly, the thermodynamic flow power was then calculated using Eq. 1.

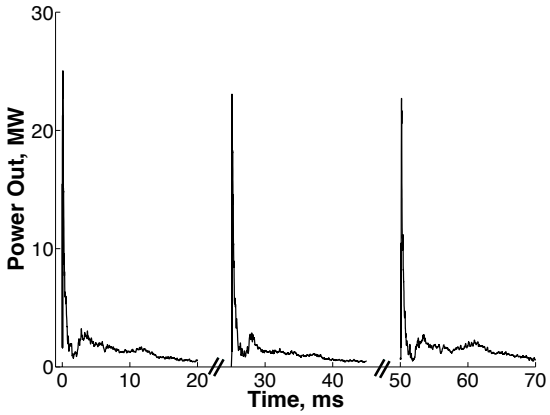

Figure 5. Time-resolved power output for three consecutive PDC cycles.

$$P = \dot{m}(h_{sensible,mix} + \frac{1}{2}u^2) \qquad \text{(Eq. 1)}$$

Here P is the thermodynamic flow power, $\dot{m}$ is the mass flow rate, $h_{sensible,mix}$ is the mass-specific sensible enthalpy of the mixture relative to 298 K, and u is the bulk flow speed. Figure 5 shows that the NPS PDC consistently produced a peak flow power near 25 MW.

5 Summary

A TDLAS sensor for temperature and H_2O measurements in high-pressure and high-temperature combustion gases has been designed, constructed, and demonstrated. This sensor was calibrated in high-pressure and high-temperature shock tube experiments, and deployed in a PDC at NPS. The observed time-varying behavior and magnitude of temperature and H_2O measurements are consistent with predictions by elementary theory and computational fluid dynamics, supporting the accuracy of the independently determined equivalence ratio. Lastly, by conducting measurements in the choked throat of the PDC exit nozzle, it is possible to calculate the time-resolved thermodynamic flow power exiting the combustor, a quantity of primary interest in the development of work extraction devices integrated downstream of a pulsed combustor.

Acknowledgements

This work was sponsored by the Air Force Office of Scientific Research (AFOSR) and Innovative Scientific Solutions Incorporated (ISSI). The authors would like to thank Professor Chris Brophy and Dave Dausen of NPS for hosting the measurement campaign and operating the PDC.

References

[1] Chang LS, Jeffries JB, Hanson RK. (2010). Mass flux sensing via tunable diode laser absorption of water vapor. AIAA J. 48: 2687.

[2] Li H, Farooq A, Jeffries JB, Hanson RK. (2007). Near-infrared diode laser absorption sensor for rapid measurements of temperature and water vapor in a shock tube. Appl. Phys. B 89: 407.

[3] Sanders ST, Baldwin JA, Jenkins TP, Baer DS, Hanson RK. (2000) Diode-laser sensor for monitoring multiple combustion parameters in pulse detonation engines. Proc. Combust. Inst. 28: 587.

[4] Spearrin RM, Goldenstein CS, Jeffries JB, Hanson RK. (2013) Mid-infrared laser absorption diagnostics for detonation studies. Submitted to ISSW 29, Madison, WI.

[5] Rieker GB, Jeffries JB, Hanson RK. (2009). Calibration-free wavelength-modulation spectroscopy for measurements of gas temperature and concentration in harsh environments. Appl. Optics. 48: 5546

[6] Kluczynski P., Axner, O. (1999). Theoretical description based on Fourier analysis of wavelength modulation spectrometry in terms of analytical background signals. Appl. Optics. 38: 5803

[7] Bomse DS, Stanton AC, Silver, JA. (1992). Frequency modulation and wavelength modulation spectroscopies: comparison of experimental methods using a lead-salt diode laser. Appl. Optics. 31: 718.

[8] Zhou X, Jeffries JB, Hanson RK. (2005). Development of a fast temperature sensor for combustion gases using a single tunable diode laser. Appl. Phys. B. 81: 711

[9] Goldenstein CS, Schultz IA, Jeffries JB, Hanson RK. (2012). TDL absorption sensor for temperature measurements in high-pressure and high-temperature gases. AIAA Aerospace Sciences Meeting. AIAA-2012-1061, Nashville.

[10] Petersen EL, Hanson RK. (2001). Nonideal effects behind reflected shock waves in a high-pressure shock tube. Shock Waves. 10: 402

[11] Varghese PL. (1983). Tunable infrared diode laser measurements of spectral parameters of carbon monoxide and hydrogen cyanide. Doctoral dissertation. Stanford University.

[12] Li H, Farooq A, Jeffries JB, Hanson RK. (2008). Diode laser measurements of temperature-dependent collisional-narrowing and broadening parameters of Ar-perturbed H2O transitions at 1391.7 and 1397.8nm. J Quant Spectrosc Ra. 109: 132

[13] Ben-Dor G, Igra O, Elperin T. (2000). Handbook of shock waves. Chap. 3-4. Academic Press, San Diego.

[14] Burcat A, Branko R. (2005). Third millennium ideal gas and condensed phase thermochemical database for combustion with updates from active thermochemical tables. Technical Report ANL-05/20 TAE 960, Argonne National Laboratory and Technion Israel Institute of Technology.